TOTAL GASEOUS RADIATION MODELING FOR NATURAL GAS COMBUSTION WITH FULL-RANGE HYDROGEN BLENDING RATIOS BASED ON LINE BY LINE METHOD

Guopei JIN; Shiquan SHAN*; Jinhong YU; Zhihua Wang; Zhijun ZHOU

State Key Laboratory of Clean Energy Utilization, Zhejiang University, Hangzhou 310027, China

Corresponding authors Emails: shiquan1204@zju.edu.cn; shiquan1204@163.com

Hydrogen-blended combustion is recognized as a crucial pathway for hydrogen utilization and is suitable for gas turbines and boilers. Under such conditions, the H_2O/CO_2 molar ratio in the flue gas varies significantly, resulting in changes to thermal radiative properties. Accurate heat transfer calculations require new reference data and updated computational methods, especially for high-temperature and high-pressure condition. This study proposes a novel total radiation model based on the weighted-sum-of-gray gases (WSGG) principle, tailored for natural gas combustion with full-range hydrogen blending ratios (0-100%), introducing an innovative weighting coefficient formulation to account for pressure (1-40 atm), temperature (400-2500 K), and H_2O/CO_2 molar ratio effects on radiative properties. The model, benchmarked against the HITEMP 2010 based line by line (LBL) method, covers the partial pressure path lengths from 0.001 to 60 atm·m. The accuracy of the new WSGG model was validated through emissivity calculations and one- and two-dimensional radiative heat transfer simulations, while the impacts of pressure, gas composition, and path length on radiative heat transfer were investigated. The average heat source error does not exceed 4.18% under full working conditions. The developed model provides a critical foundation for designing hydrogen-blended natural gas combustors and CFD-based calculations.

Keywords: *WSGG model; Radiative heat transfer; Hydrogen blended fuel; Line by line method; Radiative modeling*

1 Introduction

Thermal engineering relies on fuel combustion to achieve energy conversion and power generation, with typical systems including gas turbines and boilers. Fossil fuel-based thermal engineering technologies have been extensively developed and widely applied. However, the large-scale and continuous use of fossil energy has caused a series of problems, such as energy

crises, the greenhouse effect, and air pollution. Therefore, the development of clean fuels and advanced energy technologies have received significant attention. The integrated and efficient utilization of hydrogen, ammonia, and other common carbon-free energy sources is critical for achieving carbon neutrality [1]. Among these, hydrogen-blended natural gas combustion combines the merits of natural gas and hydrogen has emerged as a promising pathway for deep decarbonization. Due to the potential to significantly reduce carbon emissions, the utilization of hydrogen-blended natural gas could therefore see widespread development in industries, buildings, and transportation where emission reductions are typically challenging. At present, the thermal utilization of hydrogen-blended fuels has entered the stage of practical application in many countries and regions, including scenarios such as gas turbines and boilers. Numerous in-depth studies have been conducted on the flame structure, combustion characteristics, and emissions of hydrogen-blended fuels, concluding that the addition of hydrogen can reduce dependence on fossil fuels, enhance energy security, and improve air quality [2].

During combustion processes, substantial thermal energy is released, producing high-temperature flames and radiatively active species such as H_2O, CO_2, NOx, and soot, all of which play a critical role in radiative heat transfer. Consequently, thermal radiation becomes dominant heat transfer mechanism in high-temperature industrial equipment [3]. In pressurized combustion applications, the influence of the medium on radiative heat transfer characteristics is even more pronounced [4]. Accurate modeling of radiative heat transfer is therefore essential for reliable prediction of combustion system temperatures [5]. Moreover, since NO formation kinetics are highly sensitive to temperature, neglecting radiation effects in combustion simulations can result in significant overestimation of NO concentrations due to indirectly affected temperature predictions [6]. Precise evaluation of gas radiation in combustion processes is vital for optimizing boiler design, ensuring operational safety, and controlling pollutant emissions. Due to distinct physical and chemical properties of hydrogen and natural gas, introducing hydrogen into natural gas can significantly alter the flame structure and radiative characteristics. Moreover, the strong coupling among turbulence, chemical reactions, and non-gray gas radiation leads to a substantial influence of radiative predictions on overall simulation results. This, in turn, highlights the need for more accurate radiation models under hydrogen-blended natural gas combustion conditions.

In engineering radiative heat transfer calculations, gas emissivity serves as a critical parameter, and the use of lookup tables remains one of the most efficient and convenient approaches for its determination. Hottel et al. [7,8] were among the first to establish emissivity charts for CO_2, H_2O, and their mixtures. Over the past several decades, a wide range of gas emissivity tables have been developed. For high-precision computational fluid dynamics (CFD) simulations, utilizing the radiation model is a more widely used method for quickly calculating thermal radiation transfer [9]. Radiation models constitute a critical sub-model in combustion simulation. In particular, the simplified weighed-sum-of-gray-gases (WSGG) model is commonly used due to its ability to provide reasonably accurate radiative heat transfer predictions while maintaining computational efficiency. Different WSGG models have been developed for various application scenarios. For conventional air combustion, Smith et al. [10] established a WSGG model suitable for temperatures of 600-2400 K and partial pressure path lengths of 0.001-10 atm·m, using an exponential wide-band model as the benchmark. For oxy-

fuel combustion. Kangwanpongpan et al. [11] developed revised parameters through line-by-line calculations based on HITEMP 2010 database, extending the H_2O/CO_2 molar ratio coverage to 0.125-4. Wu et al. [12] developed a new model additionally accounts for CO produced by incomplete combustion. Regarding pressurized environments, Shan et al. [13,14] first developed a model based on a statistical narrow band model for pressurized oxy-fuel combustion. Cai et al. [15] proposed a WSGG model for coal gasification under specific high-pressure conditions, incorporating the radiative effects of CO. Recent advances in model include architecture modifications. Wang et al. [16] incorporated total pressure into the weighting coefficients for aero engine combustors, effectively extending operational pressure range to 1-30 atm. Referring to this work, Selhorst et al. [17] incorporated H_2O/CO_2 molar ratio dependencies into the weighting coefficient formulation. Liu et al. [18] proposed an interpolation WSGG method based on the full-spectrum correlated-*k* (FSCK) approach to handle CO_2-H_2O-soot mixtures, which improved the computational efficiency of the existing superposition WSGG method without sacrificing calculation accuracy. However, in hydrogen-blended natural gas combustion, increasing hydrogen blending ratios reduce carbon emissions but alter radiation characteristics through the elevated H_2O concentrations in the flue gases, there is currently no comprehensive WSGG model that can perform complete calculations of gas radiation for natural gas with 0-100% hydrogen blending under different pressure conditions.

Against this background, a novel total radiation model has been developed based on the weighted-sum-of-gray gases (WSGG) principle, specifically tailored for hydrogen-blended natural gas combustion. Radiative behavior across the full-range hydrogen blending ratios (0–100%) under pressures of 1–40 atm is accounted for in the proposed formulation. Benchmarking is carried out against a line-by-line (LBL) model using the HITEMP 2010 database, covering path lengths of 0.001-60 atm·m and temperatures of 400-2500 K. The performance of the new WSGG model is evaluated through gas emissivity predictions and several radiative transfer test cases. Accuracy and novelty are confirmed by comparative analyses with LBL reference data. The establishment of an efficient and accurate WSGG model for hydrogen-blended natural gas combustion is considered of significant importance for engineering design and practical applications.

2 Models and methods

2.1 LBL model

In conventional combustion industrial applications, CO_2 and H_2O are the most common gaseous media that participate in the emission and absorption of radiative energy, exhibiting strong wavelength dependence. From computational perspectives, the LBL model achieves the highest spectral resolution which involves detailed individual absorption lines of gas molecules, can provide the most accurate spectral characteristic calculations by solving the radiative transfer equation (RTE) for each spectral absorption coefficient. However, its prohibitive computational demands limit its application in real-time or large-scale simulations. Nevertheless, this method remains the gold standard for radiative modeling and serves as an

essential standard for validating alternative radiation models in combustion research.

In this study, the relevant parameters of target gases were obtained from the HITEMP 2010 database [19], focusing on the gas radiation characteristics in the infrared spectrum (0-10000 cm^{-1}). The HITEMP 2010 database incorporates and extends the CDSD-2008 database for CO_2 and the refined BT2 database for H_2O, specifically optimized for high-temperature conditions up to 3000 K. In the LBL model, the spectral absorption coefficient is formulated as [20]:

$$\kappa_\nu = N \sum_i S_i(T) F_i(\nu) \tag{1}$$

where N is the molecule number density, S_i is the spectral line intensity derived by extending the line intensity under standard conditions. F_i is the line shape function, where Lorentz line profile is applied in this work [21]:

$$F_i(\nu) = \frac{\gamma_i}{\pi[(\nu - \nu_i)^2 + {\gamma_i}^2]} \tag{2}$$

where ν_i is the central wave number of the *i*-th spectral line, γ_i is the half-width at half-maximum (HWHM) of the line due to collisional or pressure broadening:

$$\gamma_i(T, P, P_s) = \left(\frac{T_0}{T}\right)^n \left[\gamma_{\mathrm{air},i}(P_0, T_0)(P - P_a) + \gamma_{\mathrm{self},i}(P_0, T_0) P_a\right] \tag{3}$$

where P_0 and T_0 are the reference pressure and temperature, respectively. In HITEMP 2010 database, $P_0 = 1$ atm and $T_0 = 296$ K. $\gamma_{\mathrm{air},i}$ and $\gamma_{\mathrm{self},i}$ represent the air-broadened and self-broadened half-widths of the *i*-th spectral line, respectively. n is the temperature-dependence exponent for γ_{air}. All these parameters can be obtained from the HITEMP 2010 database.

To improve the computational efficiency of the LBL model, this study implements spectral line truncation by selectively eliminating weak absorption lines with negligible radiative contributions. Based on the characteristics of Lorentz line profile, the absorption coefficient contribution of spectral lines distant from the sampling point is relatively small. According to Dorigon et al. [22], cutoff distances are set to $\Delta\nu_{CO2} = 800\ \mathrm{cm}^{-1}$ and $\Delta\nu_{H2O} = 40\ \mathrm{cm}^{-1}$ for CO_2 and H_2O, respectively. By ignoring the lines beyond these distances and using a wavenumber interval of 0.067 cm^{-1} (1.5×10^5 wavenumber points in total), sufficiently accurate results can be obtained while significantly reducing the computational cost, achieving an optimal balance between accuracy and computational economy.

Total emissivity is defined as the ratio of the spectrally integrated emissive power to the spectrally integrated blackbody emissive power:

$$\varepsilon_g = \frac{\int_0^\infty \varepsilon_\lambda I_{b\lambda} d\lambda}{\int_0^\infty I_{b\lambda} d\lambda} = \frac{\pi \int_0^\infty I_{b\lambda}[1 - exp(-\kappa_\lambda L)]\, d\lambda}{\sigma T^4} \tag{4}$$

where $I_{b\lambda}$ is the spectral blackbody emissive power according to Planck law and σ is the Stefan-Boltzmann constant. All calculations were carried out on a workstation equipped with 64-Core AMD EPYC 2.2 GHz processors and 512 GB RAM. Using Parallel Computing Toolbox in MATLAB software for parallel computation acceleration. The calculation at a given thermodynamic state requires approximately 21 hours of CPU time.

2.2 WSGG model

Global radiative models aim to directly obtain the total radiative intensity through full-spectrum without considering the spectral details. In contrast to LBL models that calculates the spectral intensity $I_\eta(s,\boldsymbol{\Omega})$, the primary goal of the global model is to directly determine the total radiative intensity:

$$I = I(s,\boldsymbol{\Omega}) = \int_0^\infty I_\eta(s,\boldsymbol{\Omega})d\eta \tag{5}$$

The WSGG model is a widely used global model that is compatible with any radiative transfer solution method and is easy to couple with computational fluid dynamics (CFD) software. Initially proposed by Hottel and Sarofim [8], the model simplifies the WSGG model simplifies the radiative heat transfer calculation by approximating the complex radiative properties of non-gray gases as a weighted sum of multiple gray gases. The gas emissivity in WSGG model is formulated as:

$$\varepsilon_g = \frac{1}{I_b(T)}\int \varepsilon_\eta I_{b\eta}(T) \approx \sum_{i=1}^{J_g} w_{g,i_g}(T)\left[1 - exp\left(-\kappa_{g,P,i_g}XPL\right)\right] \tag{6}$$

where w_{g,i_g} and κ_{g,P,i_g} are the weight and absorption coefficient of the *i*-th gray gas, respectively. P is total pressure, L is the path length, X is the volume fraction of the radiating gas.

The partial pressure of the radiating gas P_a is expressed as:

$$P_a = P_{\mathrm{H_2O}} + P_{\mathrm{CO_2}} \tag{7}$$

where $P_{\mathrm{H_2O}}$ and $P_{\mathrm{CO_2}}$ represent the partial pressures of H_2O and CO_2, respectively. Building upon the methodological framework established by Johansson et al. [23] and Bordbar et al. [24], this study adopts a WSGG model with 4 gray gases. The benchmark emissivity data is generated using the LBL model over a temperature range of 400-2500 K and a partial pressure path length range of 0.001-60 atm·m, which is used to fit the parameters of the WSGG model.

To enable precise computation of radiative models for natural gas combustion gases across full hydrogen blending ratios, the model was modified by simultaneously incorporating both temperature (*T*) and molar ratio (*M*) into the weighting coefficients:

$$w_{g,i_g}(T,M) = a_{i_g}(T)b_{i_g}(M) \tag{8}$$

where

$$a_{i_g}(T) = \sum_{j=0}^{5}\alpha_{i_g,j}\left(\frac{T}{T_{ref}}\right)^j \tag{9}$$

$$b_{i_g}(M) = \sum_{j=0}^{3}\beta_{i_g,j}\left(\frac{M}{M_{ref}}\right)^j \tag{10}$$

where $\alpha_{i_g,j}$ and $\beta_{i_g,j}$ are polynomial coefficients. To improve the accuracy of the polynomial, the reference temperature $T_{\mathrm{ref}} = 2000$ K, and the reference molar ratio $M_{\mathrm{ref}} = 3$.

Direct extension of atmospheric WSGG models to elevated pressure conditions is proved to introduce significant errors [25]. To make the WSGG model applicable to a wide range of pressure conditions, this study further represents the gray gas absorption coefficient κ_{g,i_g}, the

temperature polynomial coefficient $\alpha_{i_g,j}$, and the pressure polynomial coefficient $\beta_{i_g,j}$ as quadratic functions of pressure P:

$$\kappa_{g,P,i_g} = K0_{i_g} + K1_{i_g}P + K2_{i_g}P^2 \tag{11}$$

$$\alpha_{i_g,j} = A0_{i_g,j} + A1_{i_g,j}P + A2_{i_g,j}P^2 \tag{12}$$

$$\beta_{i_g,j} = B0_{i_g,j} + B1_{i_g,j}P + B2_{i_g,j}P^2 \tag{13}$$

To enable efficient and accurate numerical simulations of hydrogen-blended natural gas combustion, a new WSGG model was established to cover radiative characteristic calculations across full hydrogen-blending ratios. The molar ratio range was set to 2-∞ to encompass 0-100% hydrogen blending fractions. However, due to practical limitations in the model structure, the upper limit of the molar ratio was set to 10. Subsequent validation demonstrated that the radiative transfer results for $M = 10$ are close to the $M = \infty$ case. The main WSGG parameters were optimized through sequential quadratic programming (SQP) coupled with polynomial fitting. Detailed parameters are provided in Table 1.

Table 1

Gas WSGG coefficients

i_g	K0 ($atm^{-1} \cdot m^{-1}$)	K1 ($atm^{-1} \cdot m^{-1} \cdot atm^{-1}$)	K2 ($atm^{-1} \cdot m^{-1} \cdot atm^{-2}$)
1	5.13359×10^{-2}	6.42902×10^{-5}	5.92527×10^{-6}
2	4.22120×10^{-1}	-3.45252×10^{-3}	8.90066×10^{-5}
3	3.26122×10^{0}	3.17893×10^{-2}	-6.03623×10^{-4}
4	4.32853×10^{1}	-3.40648×10^{-1}	6.73886×10^{-3}
i_g,j	A0	A1 (atm^{-1})	A2 (atm^{-2})
1,0	4.29682×10^{0}	7.40487×10^{-1}	-1.73581×10^{-2}
1,1	-6.36704×10^{0}	-3.90981×10^{0}	8.71246×10^{-2}
1,2	-7.80828×10^{0}	7.18517×10^{0}	-1.56795×10^{-1}
1,3	4.37244×10^{1}	-3.23404×10^{0}	6.63716×10^{-2}
1,4	-4.34238×10^{1}	-1.95345×10^{0}	4.61525×10^{-2}
1,5	1.31316×10^{1}	1.39873×10^{0}	-3.12274×10^{-2}
2,0	-1.81964×10^{0}	-4.43015×10^{-2}	9.17400×10^{-4}
2,1	2.30870×10^{1}	3.69379×10^{-1}	-4.12769×10^{-3}
2,2	-5.87024×10^{1}	-8.73586×10^{-1}	2.37166×10^{-2}
2,3	7.65290×10^{1}	1.42363×10^{-1}	-3.18105×10^{-2}
2,4	-4.90992×10^{1}	8.79345×10^{-1}	1.37047×10^{-2}
2,5	1.21736×10^{1}	-4.91893×10^{-1}	-9.05807×10^{-4}
3,0	1.17287×10^{0}	-2.07128×10^{-1}	3.89181×10^{-3}
3,1	1.89026×10^{1}	2.27109×10^{-1}	-6.48579×10^{-3}
3,2	-4.73238×10^{1}	3.53498×10^{-1}	-6.00612×10^{-3}
3,3	5.71491×10^{1}	-4.08943×10^{-1}	7.56627×10^{-3}
3,4	-3.74327×10^{1}	-2.75260×10^{-1}	8.11765×10^{-3}
3,5	9.95547×10^{0}	2.69385×10^{-1}	-6.88085×10^{-3}

4,0	1.25780×10^{1}	-1.0994×10^{0}	2.18608×10^{-2}
4,1	-3.48821×10^{0}	1.00184×10^{0}	-2.18415×10^{-2}
4,2	-2.74403×10^{1}	-1.15918×10^{0}	2.82153×10^{-2}
4,3	1.86684×10^{1}	4.28067×10^{0}	-8.97332×10^{-2}
4,4	6.91969×10^{0}	-4.68317×10^{0}	9.43772×10^{-2}
4,5	-5.91890×10^{0}	1.52862×10^{0}	-3.03068×10^{-2}
i_g, j	B0	B1 (atm^{-1})	B2 (atm^{-2})
1,0	1.03482×10^{-1}	-5.35868×10^{-3}	1.20205×10^{-4}
1,1	-9.51996×10^{-3}	9.37639×10^{-4}	-5.00471×10^{-6}
1,2	3.01560×10^{-3}	-4.32972×10^{-4}	1.58718×10^{-6}
1,3	-3.87289×10^{-4}	7.02407×10^{-5}	-2.48923×10^{-7}
2,0	1.17470×10^{-1}	2.24606×10^{-3}	-8.18128×10^{-5}
2,1	2.32274×10^{-2}	-8.58088×10^{-4}	5.16890×10^{-6}
2,2	-1.06958×10^{-2}	6.58899×10^{-4}	-7.74472×10^{-6}
2,3	1.69333×10^{-3}	-1.29746×10^{-4}	1.76187×10^{-6}
3,0	5.50150×10^{-2}	3.37660×10^{-3}	-1.58983×10^{-5}
3,1	2.60212×10^{-2}	-1.00065×10^{-3}	2.37321×10^{-5}
3,2	-9.73061×10^{-3}	2.94805×10^{-4}	-7.83089×10^{-6}
3,3	1.26490×10^{-3}	-2.55579×10^{-5}	8.29764×10^{-7}
4,0	1.91987×10^{-2}	1.18421×10^{-2}	-2.20284×10^{-4}
4,1	-7.05085×10^{-3}	-2.62890×10^{-3}	4.78381×10^{-5}
4,2	2.43525×10^{-3}	1.06201×10^{-3}	-2.00987×10^{-5}
4,3	-3.03033×10^{-4}	-1.56480×10^{-4}	3.01251×10^{-6}

3 Investigated cases

The spatial evolution of radiation intensity I_v through participating media along a path s is governed by the radiative transfer equation (RTE), which mathematically describes the interplay of emission, absorption, and transmission of energy. For gaseous radiative transfer, scattering effects can be neglected in the calculations. The RTE for an absorbing, emitting and non-scattering gaseous medium can be expressed as:

$$\frac{dI_v}{ds} = \kappa_v I_{vb} - \kappa_v I_v \tag{14}$$

in which I_{vb} is the spectral blackbody radiative intensity. In this work, the Discrete Ordinates Method (DOM) [26] is used to solve the RTE coupled with WSGG and LBL model, using S_8 angular quadrature scheme, as detailed in [13].

Both 1-D and 2-D radiative heat transfer were investigated, the case study examines the radiative transfer of a gas medium enclosed by a blackbody surface. As shown in Table 2, for one-dimensional cases, the distance between the walls differs between 0.5 and 5 m, and the wall temperature is set to 1000 K. A grid discretization with 100 cells is employed. The hydrogen ratio denotes the volume fraction of hydrogen in hydrogen-enriched natural gas fuel. Isothermal conditions assumed uniform gas temperatures maintained at 1200 K, while non-isothermal conditions imposed a cosine-distributed temperature profile as:

$$T(x) = 1400 - 400\,cos(\frac{2\pi x}{L}) \quad \text{(K)} \tag{15}$$

where x is the position and L is the distance between the walls. For the non-homogenous case, the molar fraction of H_2O is assumed as:

$$\mathrm{X}_{H_2O}(x) = 0.5 + 0.2\cos\left(\frac{2\pi x}{L}\right) \tag{16}$$

Radiative heat transfer is evaluated primarily through the determination of the radiative heat flux q and radiative heat source $\dot{q}$ at position x, which are expressed as follows:

$$q(x) = \sum_i \sum_l 2\pi\mu_l w_l [I_i^+(x,l) - I_i^-(x,l)] \tag{17}$$

$$\dot{q}(x) = \sum_i \sum_l \left\{2\pi\kappa_{p,i} w_l [I_i^+(x,l) + I_i^-(x,l)] - 4\pi\kappa_{p,i} w_l I_{b,i}(x)\right\} \tag{18}$$

Here, μ_l denotes the cosine of the angle between the considered direction and the x-axis, and w_l is the corresponding weighting factor. The terms $I_i^+(x,l)$ and $I_i^-(x,l)$ represent the directional radiative intensities in the forward and backward directions, respectively.

Table 2

Cases in One-dimensional condition

Case	T (K)	Hydrogen Ratio	L (m)	M	P (atm)	$X_{\mathrm{H_2O}}$	$X_{\mathrm{CO_2}}$
Homogenous							
1.1	Eq. (15)	0%	5	2	1	0.6	0.3
1.2	Eq. (15)	50%	5	3	1	0.675	0.225
1.3	Eq. (15)	75%	5	5	1	0.75	0.15
1.4	Eq. (15)	100%	5	∞	1	0.9	0
1.5	Eq. (15)	75%	1	5	1	0.75	0.15
1.6	Eq. (15)	75%	3	5	1	0.75	0.15
1.7	1200	75%	1	5	1	0.75	0.15
1.8	Eq. (15)	75%	1	5	10	0.75	0.15
1.9	Eq. (15)	75%	0.5	5	40	0.75	0.15
Non-homogenous							
2.1	Eq. (15)	0%~75%	0.5	$\mathrm{X}_{H_2O}/\mathrm{X}_{CO_2}$	5	Eq. (16)	0.15

2-D rectangular combustion cases were designed to further verify the accuracy and adaptability of the model, as detailed in Table 3. The combustion region is defined as a fixed rectangle with dimensions of 1 m × 0.4 m and discretized using 100 × 40 computational grids. The temperature field is designed as:

$$T(x,y) = (14000x - 400)(1 - 3y_0^2 + 2y_0^3) + 800, \quad \text{for } x \le 0.1m \tag{19a}$$

$$T(x,y) = -\frac{10000}{9}(x-1)(1 - 3y_0^2 + 2y_0^3) + 800, \quad \text{for } x \ge 0.1m \tag{19b}$$

where $y_0 = |0.2 - y|/0.2$, which indicates the normalized distance from the point to the symmetry axis of the temperature field.

For further quantitative evaluation, the errors across all scenarios are defined as [27]:

$$\delta q = \frac{|q_{WSGG} - q_{LBL}|}{max|q_{LBL}|} \times 100\% \tag{20}$$

$$\delta \dot{q} = \frac{|\dot{q}_{WSGG} - \dot{q}_{LBL}|}{max|\dot{q}_{LBL}|} \times 100\% \tag{21}$$

Table 3 Cases in Two-dimensional condition

Case	T (K)	Hydrogen Ratio	M	P (atm)	X_{H_2O}	X_{CO_2}
3.1	Eq. (19)	20%	2.25	1	0.623	0.277
3.2	Eq. (19)	75%	5	1	0.75	0.15
3.3	Eq. (19)	75%	5	10	0.75	0.15

4 Results and discussion

4.1 Emissivity results

A comparison with the LBL method has been performed to validate the accuracy of the new model. Emissivity was calculated for various temperatures, total pressures, and path lengths using a one-dimensional uniform gas column. Fig. 1(a) presents the emissivity under different pressures, while Fig. 1(b) shows the emissivity for different H_2O/CO_2 molar ratios. It is evident that variations in pressure and composition influence the radiative properties of the gas. An increasing trend in emissivity is observed with rising total pressure, as pressure broadening of spectral lines enhances the radiative capability of the gas. Similarly, an increase in the H_2O/CO_2 molar ratio leads to higher radiative intensity of the mixture due to the greater contribution of water vapor. The results indicate that the WSGG model developed in this study maintains high accuracy in emissivity calculations across all investigated conditions, with the maximum error of the calculated points not exceeding 2.9%. This confirms the reliability of the WSGG model for emissivity predictions.

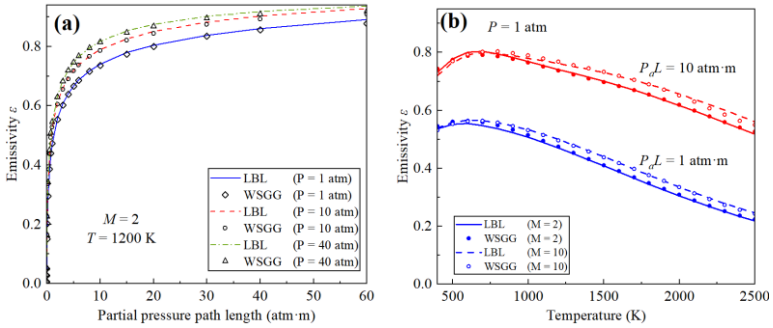

Fig. 1. Comparative analysis of gas emissivity results from WSGG and LBL Models: (a) Under varying pressure conditions; (b) With different H_2O/CO_2 molar ratios

4.2 Results of 1-D cases

The conditions for atmospheric pressure and $M = \infty$ were evaluated, where the fuel was pure hydrogen and the combustion gas product was only H_2O, shown in Fig. 2. $M = 10$ was selected as the input value for the model proposed in this study, and the results were compared with those of $M = \infty$, obtained through the LBL method. Additionally, the performance of the models proposed by Smith et al. [10], Yin et al. [28] and Shan et al. [14], all designed for

atmospheric pressure conditions, was also verified. Among them, the model of Smith et al. is a widely used typical model in CFD simulations, while the model of Yin et al. is primarily developed for oxy-fuel flames. The results show that the calculations using the new model with $M = 10$ are close to the $M = \infty$ LBL benchmark results, indicating that the model coefficients with $M = 10$ can be used to approximately calculate the radiation characteristics of pure H_2O. However, certain difference is observed in the results of the other models.

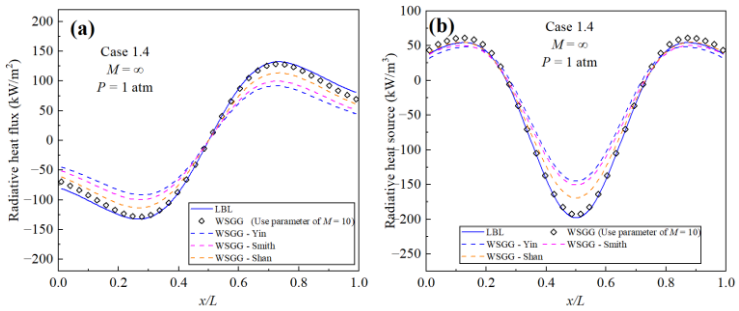

Fig. 2. Results of the Case 1.4 with different WSGG models and LBL benchmark model: (a) Radiative heat flux; (b) Radiative heat source.

Fig. 3 further examines the non-isothermal and homogenous cases by comparing the results of the new WSGG model under atmospheric and pressurized conditions, with a molar ratio of 5 representing a high 75% hydrogen blending ratio. The two cases considered different wall distances of 1 m and 0.5 m, which allow for a better assessment of the general applicability of the model. The results show that the results from the new model are quite close to those of the benchmark model, with average heat source errors of only 4.18% and 2.31%, respectively. This indicates that the new model demonstrates good accuracy and adaptability across different pressure conditions. The increase in pressure enhances the peak intensities of both the radiative heat flux and heat source. Especially for the radiative heat source, the peak value increases from -590.1 kW/m^3 under atmospheric pressure to -2261.4 kW/m^3 at 40 atm, highlighting the significant influence of pressure on radiative heat transfer. Therefore, simply applying an atmospheric pressure model is insufficient for pressurized conditions, as it would lead to significant errors.

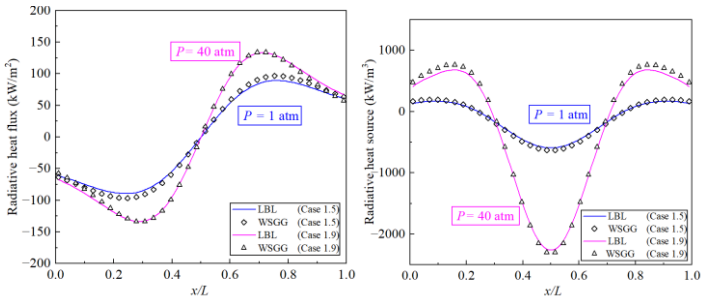

Fig. 3. Effect of pressure on radiative heat transfer: (a) Radiative heat flux; (b) Radiative heat source.

Fig. 4 illustrates the case of non-isothermal and non-homogeneous conditions, which are commonly encountered in practical applications where gas composition is unevenly distributed across different regions. In Case 2.1, the pressure is fixed at 5 atm, with the molar fraction of CO_2 maintained at 0.15, while the molar fraction of H_2O varies according to Eq. (16). Under this configuration, the molar ratio of the gas mixture ranges from 2 to 4.67, exhibiting a wide variation. The results demonstrate that the new WSGG model achieves good accuracy, with

average heat flux error and source term error controlled within 2.74% and 2.87%, respectively. These two sets of verifications for pressure and molar ratio indicate that, although some errors may arise due to the WSGG model being generated based on relatively broad molar ratio and pressure benchmarks, the overall accuracy remains within an acceptable range for engineering calculations. Therefore, the proposed comprehensive WSGG model for the hydrogen-blended natural gas combustion is considered to be of practical significance for engineering applications.

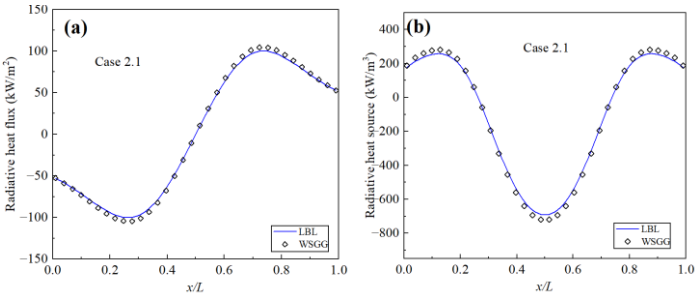

Fig. 4. Results of the Case 2.1 with the new WSGG model and LBL benchmark model: (a) Radiative heat flux; (b) Radiative heat source.

Fig. 5 evaluates the model performance under varying path lengths, considering cases of 1 m (Case 1.5), 3 m (Case 1.6), and 5 m (Case 1.3), all at atmospheric pressure with a fixed H_2O/CO_2 molar ratio of 5. The results indicate that, under atmospheric pressure, the radiative heat flux increases slightly with increasing path lengths, although the change is not significant. In contrast, a pronounced reduction in the radiative heat source is observed. In particular, when L = 1 m, the radiative heat source is considerably higher than that at longer path lengths, suggesting that radiation strongly influences the heat transfer process in short paths and cannot be neglected in the combustion simulations. Furthermore, the calculation accuracy of the new WSGG model improves as path length increases, with the average heat flux error decreasing from 5.65% to 1.98%, and the average heat source error decreasing from 4.18% to 2.82%.

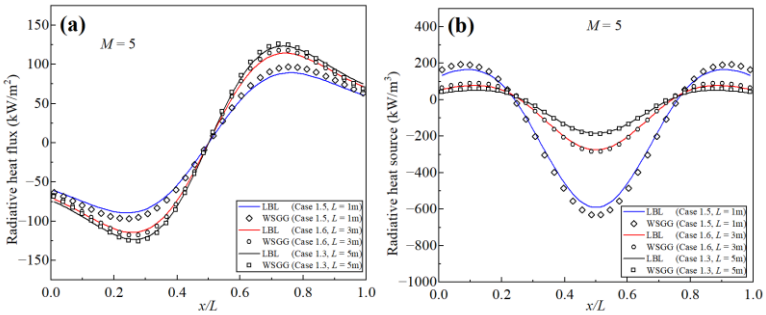

Fig. 5. Effect of path length on radiative heat transfer: (a) Radiative heat flux; (b) Radiative heat source.

Table 4 organized the heat flux and heat source errors of all 1-D test cases. In all cases, the average heat flux error does not exceed 5.65%, and the average heat source error does not exceed 4.18%, demonstrates its suitability and accuracy for engineering applications involving partially hydrogen-blended natural gas combustion.

Table 4

WSGG errors in one-dimensional cases

Errors (%)	δq_{wall}	δq_{avg}	$\delta \dot{q}_{mid}$	$\delta \dot{q}_{avg}$
Homogenous				

Case 1.1	5.12	2.41	4.46	3.40
Case 1.2	5.09	2.16	3.47	3.05
Case 1.3	5.18	1.98	2.66	2.82
Case 1.4	8.61	3.73	2.16	2.31
Case 1.5	2.62	5.65	7.22	4.18
Case 1.6	4.08	2.28	4.05	3.26
Case 1.7	1.70	1.03	0.24	0.92
Case 1.8	5.58	1.81	1.84	2.31
Case 1.9	7.59	2.48	2.62	2.56
Non-homogenous				
Case 2.1	0.02	2.74	4.63	2.87

4.3 Results of 2-D cases

This section discusses the radiative heat transfer in 2-D cases. As shown in Fig. 6, the results prove the consistency of the radiative heat source calculated using the WSGG model proposed in this work and the benchmark LBL model, under atmospheric pressure (Case 3.2) and pressurized conditions (Case 3.3), with a H_2O/CO_2 molar ratio of 5.

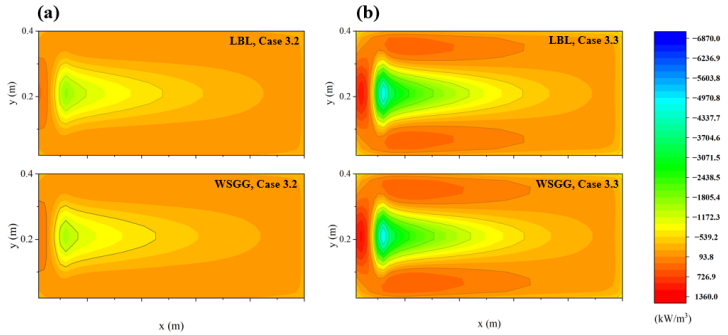

Fig. 6. Contour plots of radiative heat source in 2-D cases for different pressures: (a) Case 3.2; (b) Case 3.3.

The analysis then focused on examining the radiative heat flux and radiative source term distributions along the $x = 0.1$ and $y = 0.2$ cross-sections. These locations were selected as they represent the temperature field boundary along the x-direction and the symmetric centerline along the y-axis, where significant variations in radiative transfer occur, and the radiative source terms are relatively large and exhibit notable changes. As shown in Fig. 7, the results at these two cross-sections, demonstrating the consistency by the two models. Similar to the 1-D cases, the pressure has a significant influence on radiative heat transfer. Pressurization leads to an increase in the radiative heat source. Particularly for the $x = 0.1$ cross-section, the peak radiative source term under normal pressure was -1328.8 kW/m³, while under a pressure of 10 atm, the strongest radiative source term reached -3609.3 kW/m³, an increase of more than 2.7 times.

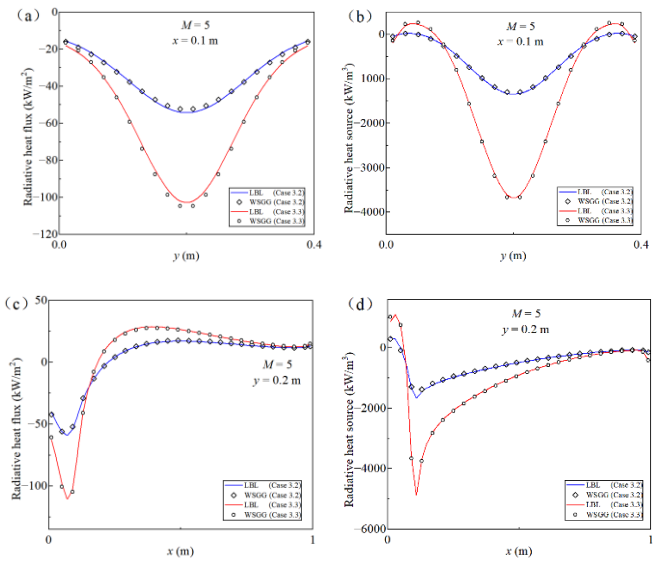

Fig. 7. Comparison of radiation heat flux and source terms by new WSGG and LBL models in 2-D cases at sections: (a) x = 0.1 (heat flux); (b) x = 0.1 (source term); (c) y = 0.2 (heat flux); (d) y = 0.2 (source term).

According to the error between the two models summarized in Table 5, the average heat flux and source term errors on these two sections do not exceed 2%. At the special position (0.1, 0.2) with the maximum absolute value of the source term, the error also does not exceed 2%.

Table 5

WSGG errors in two-dimensional cases

Errors (%)	δq_{avg}		$\delta \dot{q}_{avg}$		$\delta \dot{q}$	
	x = 0.1	y = 0.2	x = 0.1	y = 0.2	(0.1,0.2)	(0.5,0.2)
Case 3.1	0.85	0.63	0.89	0.95	1.17	0.41
Case 3.2	1.37	0.69	0.71	1.17	1.95	0.72
Case 3.3	1.39	0.64	0.69	0.45	1.16	0.38

5 Conclusions

Hydrogen-blended natural gas combustion represents an important strategy for hydrogen energy utilization and offers an economically viable pathway for energy transition. To enable accurate evaluation of the radiative characteristics of hydrogen-blended natural gas across the full hydrogen blending range (0–100%) and under varying pressures, the development of a tailored WSGG model is required. In the present work, a new WSGG model has been established and benchmarked against a line-by-line (LBL) model based on the high-resolution HITEMP 2010 database. The proposed model was applied to emissivity calculations as well as one-dimensional and two-dimensional radiative heat transfer cases, with its accuracy validated through comparisons with the benchmark LBL model. The test cases encompass a variety of H_2O/CO_2 molar ratios, pressures, and path lengths. The results demonstrate that the new model exhibits close agreement with the benchmark model. Based on the above findings, the following

conclusions can be drawn:

(1) In this study, a total gaseous radiation model for hydrogen-blended natural gas combustion under pressurized conditions has been established. Advanced expression form of weighting coefficient is adopted in the WSGG model, enabling the influence of molar ratio, pressure, and temperature to be considered while avoiding the errors introduced by additional linear interpolation.

(2) As an alternative to the emissivity lookup table method, a new global radiation model based on WSGG principle was developed in this study based on the established emissivity table, which is more suitable for CFD simulations. The WSGG model developed in this study is applicable to hydrogen-blended natural gas combustion across the entire hydrogen blending range (0–100%), under pressures of 1–40 atm, partial pressure path lengths of 0.001–60 atm·m, and temperatures of 400–2500 K.

(3) The proposed WSGG model was validated through emissivity and radiative heat transfer cases, demonstrating a high level of consistency with the benchmark LBL method results. In all investigated 1-D cases, the average heat flux error does not exceed 5.65%, and the average heat source error does not exceed 4.18%. As for the 2-D cases, the average heat flux and source term errors on the two representative sections do not exceed 2%. The increase in pressure will significantly enhance the effect of radiative heat transfer. The model developed in this study provides a foundation for the design and CFD simulation of natural gas combustion furnaces with hydrogen blending.

Acknowledgement

This work was supported by National Key Research and Development Program of China (2022YFB4003902), National Natural Science Foundation of China (52206175), Fundamental Research Funds for the Central Universities (2022ZFJH04), Scientific Research Fund of Zhejiang Provincial Education Department (Y202457107) and Natural Science Foundation of Zhejiang Province (LQZSZ24E060002).

References

[1] Dulta K, Adeola A O, Ashaolu S E, et al. Biohydrogen production and its bioeconomic impact: a review[J]. Waste Disposal & Sustainable Energy, 2022, 4(3): 219-230.
[2] Wang G, Ogden J M, Nicholas M A. Lifecycle impacts of natural gas to hydrogen pathways on urban air quality. International Journal of Hydrogen Energy, 2007, 32(14): 2731-2742.
[3] Gray W A, Kilham J K, Müller R. Heat transfer from flames. NASA STI/Recon Technical Report A, 1976, 77: 19244.
[4] Wang X, Shan S, Wang Z, et al. Review on thermal-science fundamental research of pressurized oxy-fuel combustion technology. Frontiers in Energy, 2024, 18(6): 760-784.
[5] Viskanta R, Mengüç M P. Radiation heat transfer in combustion systems. Progress in Energy and Combustion Science, 1987, 13(2): 97-160.
[6] Xu J, Huang D, Chen R, et al. An improved no prediction model for large eddy simulation of turbulent combustion. Flow, Turbulence and Combustion, 2021, 106(3): 881-899.
[7] Hottel H C, Egbert R B. Radiant heat transmission from water vapor. Transactions of the American Institute of Chemical Engineers, 1942, 38(3): 0531–0568.
[8] Hottel H C, Sarofim A F. Radiative transfer. McGraw-Hill, 1967.
[9] Bergman T L. Fundamentals of heat and mass transfer. John Wiley & Sons, 2011.
[10] Smith T F, Shen Z F, Friedman J N. Evaluation of coefficients for the weighted sum of gray

gases model. ASME Journal of Heat and Mass Transfer, 1982, 104(4): 602-608.
[11] Kangwanpongpan T, França F H R, da Silva R C, et al. New correlations for the weighted-sum-of-gray-gases model in oxy-fuel conditions based on HITEMP 2010 database. International Journal of Heat and Mass Transfer, 2012, 55(25-26): 7419-7433.
[12] Wu X, Fan W, Liu S, et al. A new WSGGM considering CO in oxy-fuel combustion: A theoretical calculation and numerical simulation application. Combustion and Flame, 2021, 227: 443-455.
[13] Shan S, Zhou Z, Chen L, et al. New weighted-sum-of-gray-gases model for typical pressurized oxy-fuel conditions. International Journal of Energy Research, 2017, 41(15): 2576-2595.
[14] Shan S, Qian B, Zhou Z, et al. New pressurized WSGG model and the effect of pressure on the radiation heat transfer of H_2O/CO_2 gas mixtures. International Journal of Heat and Mass Transfer, 2018, 121: 999-1010.
[15] Cai X, Shan S, Zhang Q, et al. New WSGG model for gas mixtures of H_2O, CO_2, and CO in typical coal gasifier conditions. Fuel, 2022, 311: 122541.
[16] Wang B, Xuan Y. An improved WSGG model for exhaust gases of aero engines within broader ranges of temperature and pressure variations. International Journal of Heat and Mass Transfer, 2019, 136: 1299-1310.
[17] Selhorst A H B, Fraga G C, Coelho F R, et al. A compact WSGG formulation to account for inhomogeneity of H_2O–CO_2 mixtures in combustion systems. ASME Journal of Heat and Mass Transfer, 2022, 144(7): 071301.
[18] Liu G, Zhu J, Liu Y, et al. A full-spectrum correlated K-distribution based interpolation weighted-sum-of-gray-gases model for CO_2-H_2O-soot mixture. International Journal of Heat and Mass Transfer, 2023, 210: 124160.
[19] Rothman L S, Gordon I E, Barber R J, et al. HITEMP, the high-temperature molecular spectroscopic database. Journal of Quantitative Spectroscopy and Radiative Transfer, 2010, 111(15): 2139-2150.
[20] Taine J. A line-by-line calculation of low-resolution radiative properties of CO_2-CO-transparent nonisothermal gases mixtures up to 3000 K. Journal of Quantitative Spectroscopy and Radiative Transfer, 1983, 30(4): 371-379.
[21] Chu H, Gu M, Consalvi J L, et al. Effects of total pressure on non-grey gas radiation transfer in oxy-fuel combustion using the LBL, SNB, SNBCK, WSGG, and FSCK methods[J]. Journal of Quantitative Spectroscopy and Radiative Transfer, 2016, 172: 24-35.
[22] Dorigon L J, Duciak G, Brittes R, et al. WSGG correlations based on HITEMP2010 for computation of thermal radiation in non-isothermal, non-homogeneous H_2O/CO_2 mixtures. International Journal of Heat and Mass Transfer, 2013, 64: 863-873.
[23] Johansson R, Andersson K, Leckner B, et al. Models for gaseous radiative heat transfer applied to oxy-fuel conditions in boilers. International Journal of Heat and Mass Transfer, 2010, 53(1-3): 220-230.
[24] Bordbar M H, Węcel G, Hyppänen T. A line by line based weighted sum of gray gases model for inhomogeneous CO_2–H_2O mixture in oxy-fired combustion. Combustion and flame, 2014, 161(9): 2435-2445.
[25] Chu H, Liu F, Zhou H. Calculations of gas thermal radiation transfer in one-dimensional planar enclosure using LBL and SNB models. International Journal of Heat and Mass Transfer, 2011, 54(21-22): 4736-4745.
[26] Chandrasekhar S. Radiative transfer. Courier Corporation, 2013.
[27] Cassol F, Brittes R, França F H R, et al. Application of the weighted-sum-of-gray-gases model for media composed of arbitrary concentrations of H_2O, CO_2 and soot. International Journal of Heat and Mass Transfer, 2014, 79: 796-806.
[28] Yin C, Johansen L C R, Rosendahl L A, et al. New weighted sum of gray gases model applicable to computational fluid dynamics (CFD) modeling of oxy−fuel combustion: derivation, validation, and implementation. Energy & Fuels, 2010, 24(12): 6275-6282.

Received: 3.10.2025.
Revised: 19.2.2026.
Accepted: 26.2.2026.